IMPROVED ELECTRODE PATTERN DESIGN FOR LATERAL FORCE INCREASE IN ELECTROSTATIC LEVITATION SYSTEM

°Shao Jü Woo*, Jong Up Jeon*, and Toshiro Higuchi*,**

*Kanagawa Academy of Science and Technology, East Block 405, KSP, 3-2-1 Sakado, Takatsu-ku, Kawasaki 213, JAPAN
Tel: +81-44-819-2093; Fax: +81-44-819-2095; E-mail: woo%naeba@intellect.pe.u-tokyo.ac.jp

**Dept. of Precision Machinery Eng., The University of Tokyo, 7-3-1 Hongo, Bunkyo-ku, Tokyo 113, JAPAN
Tel:+81-3-3812-2111 ext. 6449; Fax:+81-3-5800-6968; E-mail: higuchi@intellect.pe.u-tokyo.ac.jp

Abstract In contactless disk handling systems based on electrostatic suspension in which the stator is to be transferred, the limited stiffness in lateral direction severely restricts the achievable translational acceleration. In existing stator electrode pattern designs, the magnitude of the lateral force is determined by the magnitude of the control voltages which are applied to the individual electrodes to levitate the disk stably. As a result, the lateral force cannot be set arbitrarily.

A new stator electrode pattern is presented for the electrostatic levitation of disk-shaped objects, in particular silicon wafers and aluminum hard disks, which allows the lateral forces to be controlled independently from the levitation voltages. Therefore, greater lateral forces can be obtained, compared with the existing stator designs. Experimental results will be presented for a 4-inch silicon wafer that clearly reveal the increased lateral stiffness by using the proposed stator electrode compared to the conventional electrode pattern.

Keywords Electrostatic Suspension, Lateral Restriction Force

1. INTRODUCTION

In line with the rapid development of contactless suspension systems which has been traditionally concentrated on electromagnetic levitation, this paper deals with electrostatic levitation. Recently reported applications of electrostatic levitation concerned the contactless suspension of silicon wafers [1], aluminum hard disk media [2], and glass plates [3]. The conventional electrode patterns employed in [1-2] consist of electrodes that have the function of exerting levitation forces. Using this pattern, three degrees of freedom can be actively controlled, namely vertical motion and roll and pitch angle. The remaining degrees of freedom, among which the lateral translation, are passively stabilized through electrostatic restriction forces [4]. However, the passive lateral electric forces are an order of magnitude smaller than the levitation forces which may give rise to instability in the event of lateral disturbances. In general the lateral electric force originates from an relative lateral displacement of the levitated object with respect to the stator electrode. Increasing the stiffness in lateral direction not only but also enables electrostatic suspension to be applied in handling devices where the stator electrode is to be translated laterally over a certain range. In this case, the lateral stiffness should be large enough to accommodate the inertial forces exerted on the levitated object as a result of the translational motion.

This paper describes a method to control the lateral forces independently from the levitation forces. The basic idea is to reconfigure the electrode structure into a part which has the main function of providing levitation and one which has the main function of generating lateral forces. To accomplish the latter function, circumferential segment ring electrodes are introduced that are charged to dc high-voltages. Through this approach, the lateral forces can be controlled independently from the levitation forces by selecting the level of the dc voltages which are limited by the maximum value dictated by the break-down field strength of air. However, in vacuum environment, the break-down field strength is considerably increased so that relatively large lateral forces can be attained. A secondary function of the segment ring electrodes is to deliver a part of the bias suspension force necessary to balance the weight of the disk.

2. ORIGIN OF LATERAL FORCE

A physical explanation of the phenomenon of lateral force is given in Fig. 1. It shows two circular electrodes of which the lower electrode displays a relative translation x_d in lateral direction with respect to the other electrode.

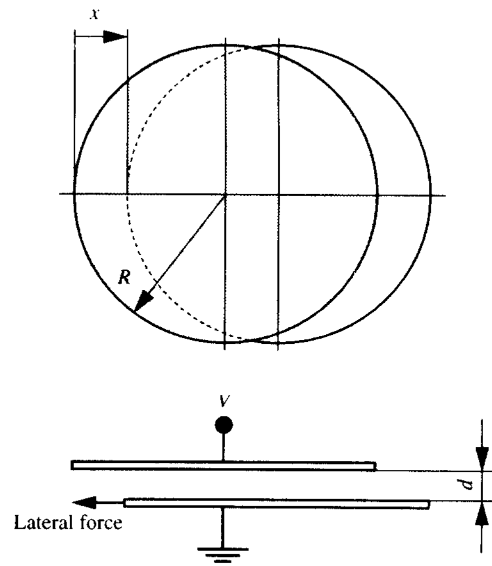

Fig. 1. Generation of lateral electric force due to lateral translation.

Due to the fringe field effects that exist between the edges of both electrodes, a restorative electrostatic force will act on the lower electrode in opposite direction of the lateral translation. This restorative force pulls the displaced electrode back to a position where both

electrodes overlap. By considering the ideal case, where the electric field between the electrodes is uniform, the following basic relation can be obtained for the lateral force F_l

$$|F_l| = \frac{\varepsilon_o \varepsilon_r V^2 (4r_d^2 - x_d^2)^{1/2}}{2d} \qquad (1)$$

where ε_o and ε_r are the permittivity of vacuum and the relative permittivity of air, respectively, d is the airgap length between the electrodes, r_d is the radius of the electrode, and V represents the voltage across the airgap.

From eqn. (1), it can be seen that the lateral force can be increased by increasing the voltage V applied across the airgap. However, in normal atmospheric conditions the break-down field strength of air, which is approximately 3 kV/mm, imposes an upper limit on V. In a vacuum environment, a break-down field strength of 15 kV/mm has been reported, so that an optimal performance of disk handling systems is expected to be found in vacuum environment.

3. STATOR ELECTRODE PATTERN DESIGN

3.1 Conventional Stator Electrode Design

Fig. 2a depicts the conventional electrode pattern which was employed to levitate a silicon wafer. It consists of four segment electrodes equally arranged to be circumscribed by a circle with the same radius as the wafer. Each segment electrode constitutes an independent force actuator and is voltage controlled by independent PID controllers. A similar type of pattern, which had a central hole, was also employed for the suspension of an aluminum hard disk [2] having an outer and inner diameter of 95 and 25 mm, respectively. A photograph of the electrode pattern is shown in Fig. 3a.

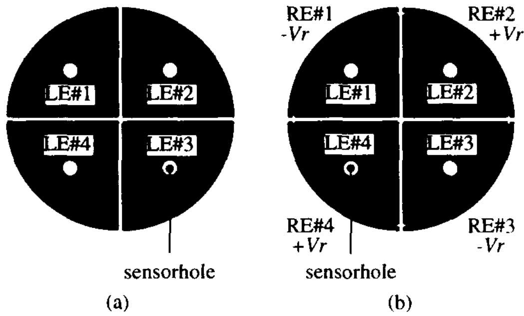

Fig. 2. (a) Conventional electrode pattern. (b) Proposed electrode pattern. Notations: LE=Levitation Electrode and RE=Ring Electrode.

3.2 Proposed Stator Electrode Design

Fig. 2b shows the proposed electrode pattern which consists of four exterior sector ring and four interior sector ring electrodes. The interior sector electrodes act as levitation electrodes and are consequently voltage controlled by PID controllers. The exterior sector ring electrodes are peripheral electrodes possessing a width of 2 mm and have the main function to exert lateral forces on the disk in the event that the latter experiences a lateral translation. These electrodes are alternately charged with dc voltages of negative and positive polarities which have the same absolute value such that the disk potential is kept to virtual ground as close as possible. Fig. 3b shows a photograph of the proposed electrode pattern.

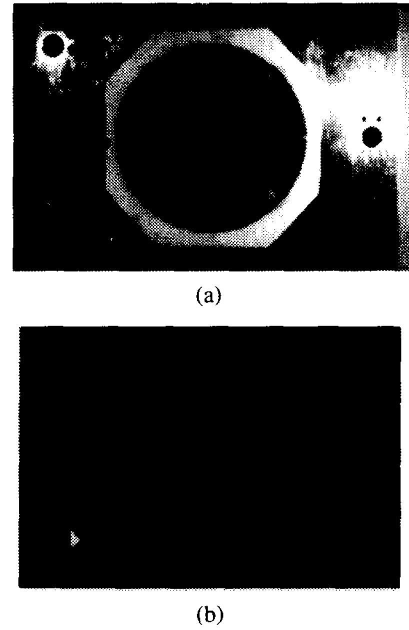

(a)

(b)

Fig. 3. Photograph of (a) Conventional electrode pattern. (b) Proposed electrode pattern.

3.3 Computation of Lateral Force

For the computation of the lateral force, the schematic diagram depicted in Fig. 4 is used. Analytically, the force exerted by the ring electrode on the wafer for a lateral translation along the x-axis can be vectorially expressed as follows:

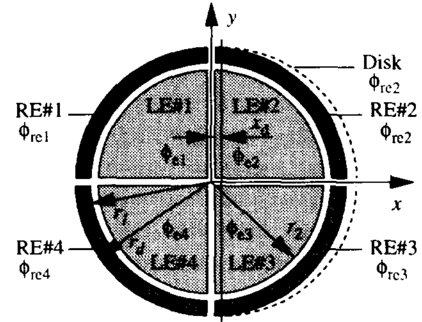

Fig. 4. Schematic diagram used for calculation of lateral force.

$$F_e\left(\phi_{le,i},\phi_{re,i},d,x_d\right) = -\frac{\partial W_e\left(\phi_{le,i},\phi_{re,i},d,x_d\right)}{\partial x_d} e_i \qquad (2)$$

where: $\phi_{le,i}$ and $\phi_{re,i}$ denote the electric potential of sector ring electrode i and sector levitation electrode i, respectively, x_d is the lateral translation of the wafer, W_d denotes the total electric field energy stored by the capacitors formed by the electrodes and the disk, e_i is the unit vector along the x-axis, and d denotes the air gap length. The energy contained in the electric field can be calculated by:

$$W_e\left(\phi_{le,i},\phi_{re,i},d,x_d\right) = \sum_{i=1}^{4} \frac{1}{2}\left(C_{re,i}\left(\phi_{re,i} - \phi_d\right)^2 + C_{le,i}\left(\phi_{le,i} - \phi_d\right)^2 \right) \qquad (3)$$

where $C_{re,i}$ represents the capacitance between ring electrode i and

the disk and $C_{le,i}$ represents the capacitance between the sector levitation electrode i and the disk. The disk potential ϕ_d can be derived as:

$$\phi_d = \frac{\sum_{i=1}^{4} C_{re,i}\phi_{re,i} + C_{le,i}\phi_{le,i}}{\sum_{i=1}^{4} C_{re,i} + C_{le,i}} \tag{4}$$

The assumption of an uniform electric field between the disk and stator offers a major simplification in the problem of determining the capacitances $C_{re,i}$ and $C_{le,i}$. As a result, these capacitances are given by the following relations:

$$C_{re,i} = \frac{\varepsilon_o \varepsilon_r A_{re,i}}{d_{re,i}}, \text{ and } C_{le,i} = \frac{\varepsilon_o \varepsilon_r A_{le,i}}{d_{le,i}} \tag{5}$$

where ε_o and ε_r are the permittivity of vacuum and the relative permittivity of air, respectively. Elaboration of eqn. (2) is performed for the interval $0 \le x_d \le 1/2(r_d - r_i)$ by using eqns. (3), (4) and (5), yielding the expression

$$\left| F_e(\partial A_{re,i}/\partial x_d) \right| = \frac{-\varepsilon_o \varepsilon_r}{2d} \sum_{i=1}^{4} (\phi_{re,i} - \phi_d)\left((\phi_{re,i} - \phi_d)\frac{\partial A_{re,i}}{\partial x_d} - 2A_{re,i}\frac{\partial \phi_d}{\partial x_d} \right) \tag{6}$$

which is a function of the following gradients

$$\frac{\partial A_{re,1}}{\partial x_d} = -(r_d^2 - x_d^2)^{1/2} \text{and} \frac{\partial A_{re,2}}{\partial x_d} = (r_d^2 - x_d^2)^{1/2} - 1/2(4r_d^2 - x_d^2)^{1/2} \tag{7}$$

where $\frac{\partial A_{re,1}}{\partial x_d} = \frac{\partial A_{re,4}}{\partial x_d}$ and $\frac{\partial A_{re,2}}{\partial x_d} = \frac{\partial A_{re,3}}{\partial x_d}$.

A further simplification can be obtained by considering an anti-symmetrical potential distribution for both the ring and levitation electrodes, i.e.,

$$\phi_{le,1} = -\phi_{le,2} = \phi_{le,3} = -\phi_{le,4} \text{ and } \phi_{re,1} = -\phi_{re,2} = \phi_{re,3} = -\phi_{re,4} \tag{8}$$

This condition leads to the aforementioned zero disk potential if the disk is exactly parallel to the stator electrodes. As a result, the expression for the electric force attains the same form as eqn. (1) where $V = |\phi_{re,1}|$.

4. EXPERIMENTAL WORK

4.1 Experimental Apparatus

Fig. 5 shows a photograph of the experimental apparatus that

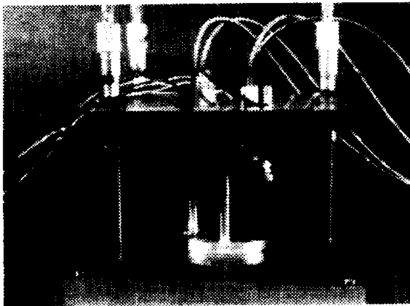

Fig. 5. Photograph of experimental levitation apparatus.

was developed for levitating a 4-inch silicon wafer. The stator electrode can be leveled using micrometer screws while the silicon wafer is supported below the stator by three micrometer screws. Fabrication of both the proposed and conventional electrode patterns were performed by etching them from a 35 μm thick copper layer on a glass-epoxy base. The areas of the individual levitation electrodes are the same and measure 17.3 cm^2 for the proposed electrode pattern and 19.6 cm^2 for the conventional electrode pattern. To measure the local airgaps at the four levitation electrodes, fiber optical sensors were installed at a radius of 33.3 mm for both patterns.

4.2 Control Strategy

A stable levitation was obtained by actively controlling the voltages applied to the levitation electrodes LE_i, where i=1~4. The feedback control structure uses the measured airgap lengths d_i, where i=1~4, between the levitation electrodes LE_i and the wafer to determine the deviations from the reference gap length. Based on these deviations, a coordinate transformation is performed to calculate the wafer position (vertical motion z) and attitude (roll angle ψ and pitch angle θ) errors. These error signals are used as feedback signals for a PID compensator whose output is transformed to the stator electrode control voltages. Subsequent addition to the four bias voltages and amplification by high voltage amplifiers, which have an amplification ratio of 1000, yield the stabilizing levitation voltages.

4.3 Experimental Results

To verify the theoretical analysis, suspension experiments have been performed using the electrode patterns shown in Figs. 2 and 3. In the following, the conventional electrode pattern is termed as electrode pattern #1 while the new electrode pattern is termed as electrode pattern #2. Both patterns were fabricated from a copper layer on a glass-epoxy base using standard etching techniques. The 4-inch silicon wafer, employed as the object of levitation, had a

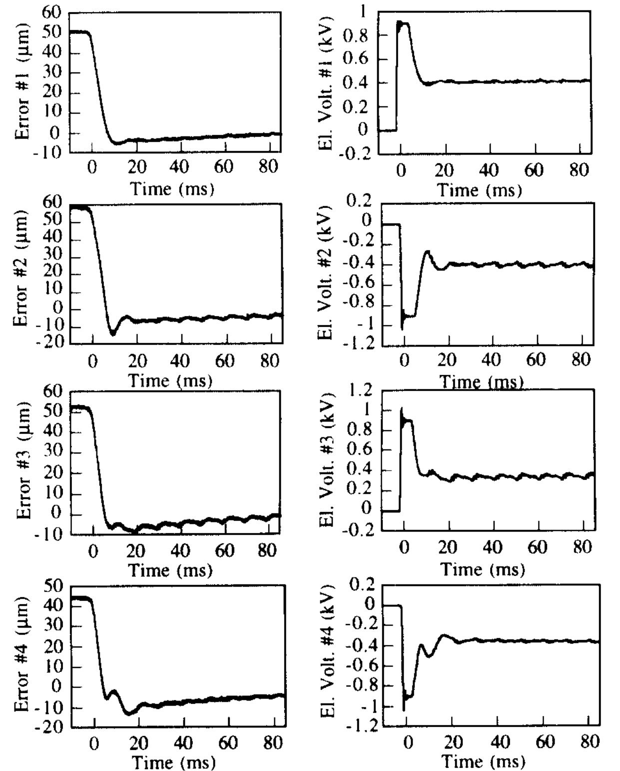

Fig. 6. Measured error signals and electrode voltage variations.

mass of 9.4 g, and a thickness of 0.7 mm. The peripheral sector ring electrodes of electrode pattern #2 were charged to dc voltages of 1.2 kV and -1.2 kV. Proportional, derivative and integral gains for the vertical movement of the wafer were respectively 10^5 kV/m, 50 kVsec/m and 10^6 kV/msec, and those for pitching and rolling are 55 kV/rad, 0.03 kVsec/rad and 10^4 kV/radsec, respectively. A bias voltage of 0.43 kV is supplied to electrode #1, #2 and #3, and -0.43 kV to electrode #4. The reference airgap was set at 300 μm. Stable suspension of the wafer was obtained for both patterns at an airgap length of 300 μm by using PID controllers. Fig. 6 shows the gap length and voltage variations for both patterns after the PID compensator was switched on.

Next, for both electrode patterns, the wafer was subjected to a small initial displacement of 1 mm. The resulting lateral oscillation was measured using a long range laser sensor. From the recorded oscillation, an estimation of the lateral stiffness was obtained. Fig. 7 and 8 show the recorded lateral response for both patterns. On the basis of the average oscillation time, which is a measure for the lateral stiffness, it was observed that pattern #2 exhibited a stiffness increase of approximately 5.5 times in comparison with pattern #1.

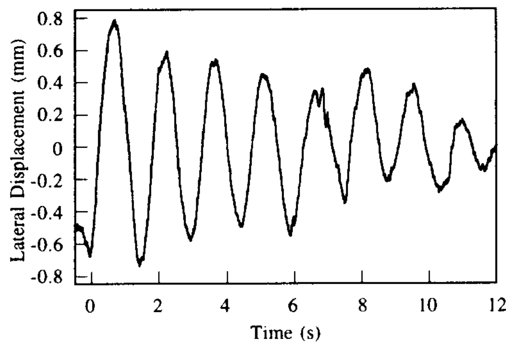

Fig. 7. Lateral displacement of wafer suspended using electrode pattern #1.

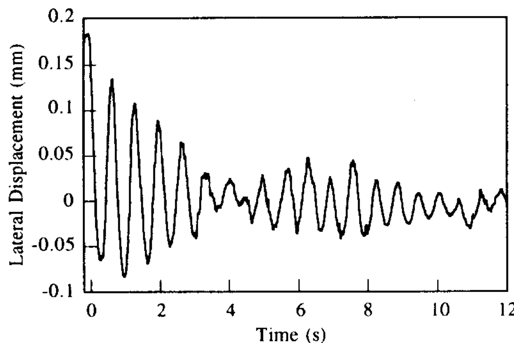

Fig. 8. Lateral displacement of wafer suspended using electrode pattern #2.

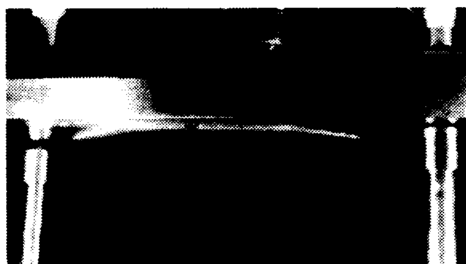

Fig. 9. Photograph of wafer in state of stable levitation.

Fig. 9 is a photograph of the wafer under stable suspension by using pattern #2.

The increase in lateral stiffness was estimated for a range of voltages that were applied to the peripheral sector ring electrodes by measuring the oscillation times. Fig. 10 shows the obtained graph.

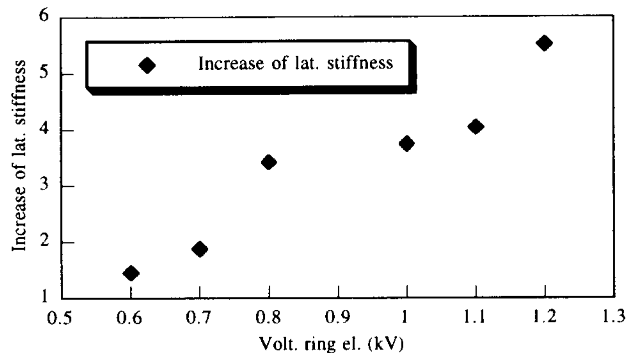

Fig. 10. Increase of lateral stiffness as a function of ring electrode voltage.

It is clear that the lateral stiffness increases as the supplied voltages to the peripheral sector ring electrodes increase. However, there is a limit to the magnitude of the supplied voltage due to instability caused by the forces and torques exerted by the peripheral sector on the levitated object. In our experiments with the silicon wafer, a sector ring electrode voltage of 1.7 kV has been attained without causing system instability to occur.

5. CONCLUSIONS

In this paper, an improved electrode pattern for contactless electrostatic suspension was described that features independent control of the lateral electric force. In conventional electrode patterns, the lateral force cannot be controlled and is therefore passive by nature. Independent control of lateral force is accomplished by subdividing the electrode pattern into two functionally distinct parts, i.e., one for providing stabilizing levitation forces and one for providing lateral forces.

Experimental validation of the proposed electrode pattern has been performed by the levitation of a 4-inch silicon wafer which shows an approximately 5.5-fold increase in lateral stiffness relative to the conventional electrode at an airgap of 300 μm and ring electrode voltage level of 1.5 kV.

REFERENCES

[1] J. Jin, T. Higuchi and M. Kanemoto, "Electrostatic Silicon Wafer Suspension", *Proc. 4th Int. Symp. Magnetic Bearings*, ETH Zurich, Switzerland, pp. 343-348, August 1994.

[2] J. Jin, T. Higuchi and M. Kanemoto, "Electrostatic Levitator for Hard Disk Media", *IEEE Trans. Industrial Electronics*, Vol. 42, No. 5, pp. 467-473, 1995.

[3] J. U. Jeon, S. J. Woo and T. Higuchi, "Electrostatic Suspension of Glass Plate", *Proc. '96 Korea Automatic Control Conference*, Pohang, South-Korea, October 1996.

[4] S. J. Woo, J. U. Jeon, T. Higuchi and J. Jin, "Electrostatic Force Analysis of Electrostatic Levitation System", *Proc. 34th SICE Annual Conf.*, International Session, Hokkaido, Japan, pp. 1347-1352, July 1995.